Available online at http://scik.org
Commun. Math. Biol. Neurosci. 2025, 2025:82
https://doi.org/10.28919/cmbn/9242
ISSN: 2052-2541

MATHEMATICAL MODELLING OF CO-INFECTION OF LASSA FEVER AND COVID-19

A. P. OLUWAGUNWA[1,*], G. M. MOREMEDI [1], S. N. NEOSSI-NGUETCHUE [2], A. S. EEGUNJOBI [2]

[1]Department of Mathematical Science, University of South Africa, South Africa

[2]Department of Mathematics, Statistics, and Actuarial Science, Namibia University of Science and Technology, Namibia

Abstract. The prevalence of Lassa fever (LF) and COVID-19 co-infections has been increasing, primarily because their modes of transmission are closely related, making individuals highly susceptible to co-infections. While there is no vaccine for LF, COVID-19 has one. Due to their significant implications, this situation necessitates implementing effective control measures to prevent a co-epidemic of these two diseases in our society. To address this, a deterministic model for LF and the COVID-19 epidemic is considered, highlighting consequences that should be addressed to avoid the challenges associated with a co-epidemic. The model undergoes qualitative analysis, and the primary reproduction number (R_0) is derived. Criteria for the stability of each model equilibrium are established. The model is numerically solved and simulated for different co-epidemic scenarios, and the findings from these simulations are discussed.

Keywords: coinfection; COVID-19; lassa fever; co-epidemi; asymptomatic.

2020 AMS Subject Classification: 92D30.

*Corresponding author

E-mail address: 21152039@mylife.unisa.ac.za

Received March 11, 2025

1. INTRODUCTION

A co-epidemic occurs when the spread of one infectious disease triggers the spread of another, such as the cases of Lassa fever (LF) and COVID-19. Studying infectious disease co-epidemics is essential for understanding the relationships between the diseases and for developing effective mathematical models for prevention and treatment efforts. This research can shed light on the complexities of infectious dynamics and inform effective control measures.

Pathogens such as bacteria, viruses, parasites, and fungi cause infectious diseases like influenza (FLU), tuberculosis (TB), HIV/AIDS, malaria, measles, hepatitis B (HB), cholera, Zika virus, Lassa fever, and COVID-19. These diseases spread from one place to another. This study aims to introduce a compartmental mathematical model to address the co-infection of COVID-19 and Lassa fever. It seeks to understand how prevention and treatment strategies can be optimized for these specific contexts.

The SAR-COV-2 virus, mostly transmitted by respiratory droplets that are released when a person that is infected talks, sneezes, coughs, or breathes, is responsible for COVID-19. It can also spread by coming into contact with contaminated surfaces, or objects, followed by touching the face, particularly the mouth, nose, or eyes. Containing the virus is challenging because it can be transmitted by asymptomatic individuals or before symptoms appear. The virus was first discovered in December 2019 in Wuhan, China's Hubei province. Its rapid global spread led to a worldwide pandemic.

The novel coronavirus emerged as a significant threat to both global public health and the economy post-World War II, surpassing the impact of two prior deadly outbreaks: the coronaviruses that cause Middle East respiratory syndrome (MERS-CoV) and severe acute respiratory syndrome (SARS-CoV) [1]. COVID-19 belongs to the class of enveloped non-segmented positive-sense, widely distributed single-stranded RNA viruses present in humans and mammals. These viruses are part of the Coronaviridae family, Ortho-coronavirinae subfamily, and Nidovirales order [2]. Following the unforeseen SARS-CoV-2 epidemic in late 2019, the global response capacity has been thoroughly tested. Human interactions have undergone lasting

changes, starting with self-isolation practices and escalating to full-scale lockdowns and quarantines to curb its transmission. Collaboratively, the scientific community has devised strategies to enhance comprehension of the ongoing crisis and promote public health measures.

Furthermore, the Lassa virus is the endemic indicator that causes Lassa fever sickness in West Africa. [3]. The primary source of Lassa infection is the multimammate rat, Mastomys natalensis, whose urine and faeces contaminate food and other objects [3, 4]. Since its discovery in Nigeria in 1969 [5], thousands of confirmed cases of Lassa fever have been reported. The disease presents with mild symptoms resembling those of malaria and typhoid fever, such as nausea, vomiting, chest pain, swollen face and cheeks, edema, dehydration, conjunctival redness, fainting spells, bleeding from bodily openings, high blood pressure, coma, and severe shock in advanced cases. Given the similarities in symptoms between COVID-19 and Lassa fever, the emergence of COVID-19 has raised significant public health concerns in Nigeria [6]. Nigeria has faced challenges in containing the pandemic since the first case was reported on February 27, 2020 (NCDC, 2020). In December 2020, Nigeria experienced a resurgence in COVID-19 cases, leading the Nigeria Centre for Disease Control (NCDC) to establish an Emergency Operations Center aimed at curbing the spread of the disease and reducing mortality rates [7].

Lassa fever is entrenched in Nigeria, with cases typically surging during the dry season from December to April and then tapering off in May [8]. The incubation period for Lassa fever ranges from one to three weeks, facilitating the spread of infection between different areas during this time [9]. The seasonal trends of Lassa fever are primarily attributed to the increased reproductive activity of the multimammate rat during the rainy season [10]. This disease was first identified in 1969 in Lassa town, Borno State, Nigeria, and later found to be endemic in Benin, Ghana, Liberia, Mali, Nigeria, Sierra Leone, and Togo [11, 12, 13]. Additionally, isolated cases of Lassa fever have been reported in the USA, Germany, the Netherlands, and Sweden. Approximately 40% of Nigeria's territory is located in areas where Lassa fever is endemic [8]. Recently, the incidence of Lassa fever has spread to 28 states and 112 Local Government Areas. From week 1 to week 37 (January to October) of 2023, there were 1068 confirmed cases

and 181 deaths reported. The majority of confirmed cases (72%) were concentrated in three states: Ondo (32%), Edo (29%), and Bauchi (11%) [14].

To halt the spread of the disease, the National Emergency Operation Center response was triggered in response to the escalating epidemiological pattern of Lassa fever since early 2022. This response has included the deployment of National Rapid Response Teams (NRRT) and the collaborative, cross-sectoral coordination of outbreak response initiatives in Nigeria [15].

It is remarkable how frequently COVID-19 and Lassa fever occur together in Nigeria. People might be hesitant to visit testing centres due to COVID-19 concerns, leading to mild or asymptomatic cases of both Lassa fever and COVID-19 [16]. This, coupled with a lack of adherence to testing protocols, significantly contributes to the under-reporting of Lassa fever cases. The similarities in clinical symptoms between COVID-19 and Lassa fever, especially in the early stages of the illness, can further lead to misdiagnoses [17]. Given Nigeria's limited healthcare resources for extensive public health interventions, this temporal overlap may have exacerbated public health and socioeconomic challenges [18].

In this context, we delve into initiatives that promote health and focus on preventing diseases. We also analyse the prevalence dynamics and study different control measures to create mathematical models. Additionally, we will discuss population-level control measures, both in combination and individually, with a strong emphasis on affordability.

For the past sixty years, mathematical modelling has proven to be a valuable research tool, providing a framework to guide decisions regarding the control of infectious diseases. Mathematical modelling involves the transformation of real-world challenges into mathematical problems, allowing for the formulation, resolution, and interpretation of outcomes using mathematical concepts. Thanks to advancements in computational capabilities, model construction, and simulation techniques, it is now more feasible than ever to model intricate physiological systems.

It furnishes the healthcare sector with a potent tool that serves two main purposes: aiding in policy formulation and facilitating decision-making. Mathematical models come in various

types, including discrete-time and continuous-time, linear or non-linear, static or dynamic. Additionally, they can be deterministic or stochastic, and empirical or physical (with equations derived from a deep comprehension of actual system characteristics) [19].

The presence of the COVID-19 pandemic has exacerbated the existing condition. As anticipated, the pandemic has had devastating impacts on public health and society wherever it has spread. This has resulted in a weakening of epidemiological control over several infectious diseases, including zoonotic ones [20, 21, 22]. Africa, like other continents, has not been spared, and the existing shortcomings in its healthcare infrastructure pose a significant disadvantage [23]. Nigeria, with other West African nations, is grappling with a recurrent outbreak of Lassa fever.

Studies indicate that a significant challenge in combating Lassa fever stems from the overlapping symptoms it shares with many other common ailments, such as sore throats, joint, back, and chest pains, and weakness [24]. The number of confirmed cases of Lassa fever surged following the emergence of COVID-19 in Nigeria. The situation is intricate because the clinical presentation of COVID-19 mirrors that of Lassa fever, heightening the risk of misdiagnosis during the initial stages of both diseases and increasing the chances of co-infection. To develop more effective healthcare strategies, it is crucial to comprehend the factors contributing to the simultaneous presence of the twin condition of COVID-19 and Lassa fever.

We have encountered several mathematical models related to COVID-19 and Lassa fever individually. However, to the best of our knowledge, no researchers have utilized mathematical modelling to explore the coexistence of COVID-19 and Lassa fever. Therefore, one of the objectives of this study is to construct a mathematical model that addresses the simultaneous presence of COVID-19 and Lassa fever.

The paper is organised as follows: Section one serves as an introduction to the topic. In section two, we propose a model of epidemiology for the co-epidemic of Lassa fever and COVID-19, illustrating the epidemic's logical progression and presenting the basic reproduction number (R_0) for the model. Finding the model's and its numerous sub-models' equilibrium solutions is the main goal of section three. Additionally, we establish criteria for assessing the local and global stability of each equilibrium point.

In the subsequent section, we will conduct a sensitivity analysis of R_0 concerning each model, solving it numerically. The numerical results will then be simulated for various co-epidemic scenarios, and the findings from these simulations will be discussed. Finally, in section five, we will present the conclusions drawn from the study.

2. MATHEMATICAL MODEL PROPOSED

The mathematical model of our consideration will divides the population of humans into five distinct and non-overlapping compartments. These compartments include: the class of people that are susceptible $S(t)$, the class of people that are only infected by Lassa fever $X(t)$, the Covid-19 only infected class $Y(t)$, the Lassa fever and Covid-19 co-infected class $Z(t)$, and the recovery class $R(t)$.

The diagram illustrating the dynamics of the Lassa fever and COVID-19 co-epidemic is depicted diagrammatically in Figure 1.

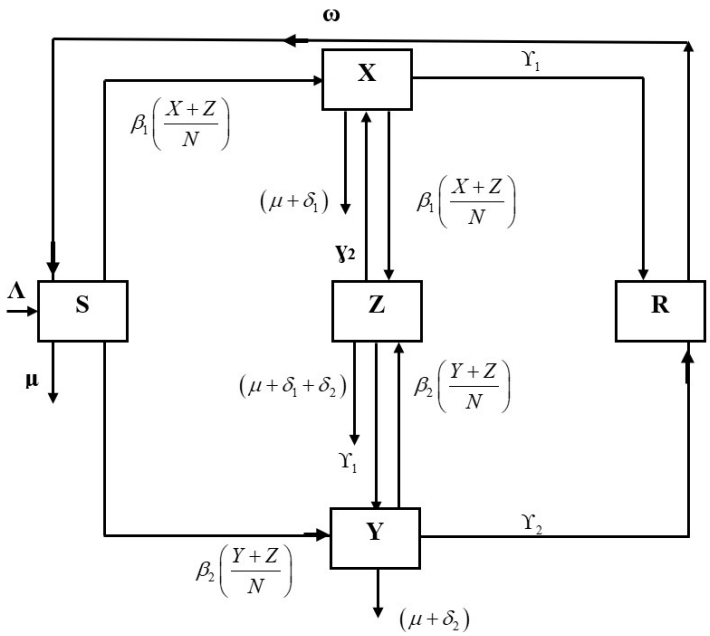

FIGURE 1. Diagram to represent the model

2.1. Basic Assumptions of the Model. Our proposed model is built upon the following assumptions, taking cues from the work of [25] and [26]:

(a) Individuals in the target population are divided into separate groups based on their infection status for each of the two diseases.

(b) The population dynamics within each of the model's compartments are entirely deterministic, and the compartments are mutually exclusive.

(c) Without distinction based on infection state, people in various compartments engage in unrestricted interaction.

(d) The natural death rate is uniform across all individuals in the various compartments, as there is no immunity to death regardless of health status.

(e) Individuals do not become infected with both diseases simultaneously; rather, they contract one disease initially and may encounter the second one subsequently.

(f) For people with one or both illnesses, all model parameters have the same numerical value and are non-negative.

(g) All new members of the population, i.e. Λ, join at a steady rate and are all susceptible.

(h) Random mixing between people in separate compartments is how diseases spread.

The dynamics of the co-epidemic involving Lassa fever and COVID-19 are represented by a system of non-linear ordinary differential equations.

TABLE 1. Description of the Model Variable

Variable	**Description**
S	Population of the susceptible humans
X	Member of those who are infected with Lassa fever only
Y	Member of those who are infected with Covid-19 only
Z	Member of those who are infected with both Covid-19 and Lassa fever infection
R	Recovery class

TABLE 2. Parameters used in the Model

Parameter	**Description**
Λ	Constant recruitment rate
ω	Temporary immunity warning rate
β_1	Transmission rate for Lassa fever
β_2	Transmission rate for Covid-19
μ	Natural death rate
γ_1	Recovery rate from Lassa fever infection
γ_2	Recovery rate from Covid-19 infection
δ_1	Disease induced death due to Lassa fever
δ_2	Disease induced death due to Covid-19

$$
\begin{aligned}
\frac{dS}{dt} &= \Lambda + \omega R - \beta_1(X+Z)\frac{S}{N} - \beta_2(Y+Z)\frac{S}{N} - \mu S \\
\frac{dX}{dt} &= \beta_1(X+Z)\frac{S}{N} - \beta_2(Y+Z)\frac{X}{N} - \mu X - \gamma_1 X - \delta_1 X + \gamma_2 Z \\
\frac{dY}{dt} &= \beta_2(Y+Z)\frac{S}{N} - \beta_1(X+Y)\frac{Y}{N} - \mu Y - \gamma_2 Y - \delta_2 Y + \gamma_1 Z \\
\frac{dZ}{dt} &= \beta_1(X+Z)\frac{Y}{N} + \beta_2(Y+Z)\frac{X}{N} - (\delta_1+\delta_2)Z - \gamma_2 Z - \gamma_1 Z - \mu Z \\
\frac{dR}{dt} &= \gamma_1 X + \gamma_2 Y - \omega R - dR
\end{aligned} \tag{1}
$$

The following represents the entire population:

$$N(t) = S(t) + X(t) + Y(t) + Z(t) + R(t) \tag{2}$$

Therefore the rate of change of the total population N(t) is obtained as follow

$$\frac{dN}{dt} = \frac{dS(t)}{dt} + \frac{dX(t)}{dt} + \frac{dY(t)}{dt} + \frac{dZ(t)}{dt} + \frac{dR(t)}{dt} \tag{3}$$

hence

$$\frac{dN}{dt} = \Lambda - \mu N \tag{4}$$

It is imperative to note that $\lim_{x\to\infty} N(t) \to \frac{\Lambda}{\mu}$. However, there is the need to show that the region Γ defined by:

$$\Gamma = \left[(S,X,Y,Z,R) \in \Re^5 | S(t)+X(t)+Y(t)+Z(t)+R(t) \leq \frac{\Lambda}{\mu}\right] \tag{5}$$

is positively invariant

We make sure that the set of equations (1) are well-posed epidemiologically. At that point, the model will have biological significance. Proving that the system is positively invariant is sufficient to illustrate this. For any time t ≥ 0, this indicates that the model predicts a positive value for each compartment. The following theorem can be used to establish this.

Theorem 1. As an attractor, the region Γ draws in any solutions that begin inside the positive orthant $\Re^1_+$.

Proof: It is evident from the equation (4), that all models, state variables, and parameters are non-negative.

$$\frac{dN}{dt} \leq \Lambda - \mu N \tag{6}$$

$$\frac{dN}{dt} + \mu N \leq \Lambda \tag{7}$$

The integrating factor exp$\int$ut therefore, by multiplying the equation (7) using an integrating factor and simplifying we obtain

$$N(t) \leq e^{ut}\left(\frac{N}{\mu}e^{ut} + c\right) \tag{8}$$

Using the initial condition i.e $N(t) = N(0)$ at $t = 0$ it implies that

$$N(t) \leq e^{-ut}\left|\frac{\Lambda}{\mu}e^{ut} + N(0) - \frac{\Lambda}{\mu}\right| \tag{9}$$

$$N(t) \leq N(0)e^{-ut} + \frac{\Lambda}{\mu}(1-e^{ut}) \implies \lim_{t\to\infty} N(t) \leq \frac{\Lambda}{\mu} \tag{10}$$

Hence, $\frac{\Lambda}{\mu}$ is the upper band of the $N(t)$ $N(t) \leq \frac{\Lambda}{\mu}$ if $N(0) \leq \frac{\Lambda}{\mu}$.

Consequently, the upper bound for the area Γ is $\frac{\Lambda}{\mu}$.

$$\Gamma = \left[(S,X,Y,Z,R) \in \Re^5 : S > 0, X > 0, X > 0, Y > 0, Z > 0, R > 0, N \leq \frac{\Lambda}{\mu}\right] \tag{11}$$

is positively invariant, indicating that the suggested model is well-posed both mathematics and epidemiologically.

2.2. Lassa Fever Sub-model. The model reduces to the Lassa fever sub-model when Covid-19 is not present (i.e., Y = 0, Z = 0). This sub-model is represented as follows:

$$\begin{aligned} \frac{dS}{dt} &= \Lambda + \omega R - \frac{\beta_1 S(X)}{S+X+R} - \mu S \\ \frac{dX}{dt} &= \frac{\beta_1 S(X)}{S+X+R} - \gamma_1 X - \mu X - \gamma_1 X \\ \frac{dR}{dt} &= \gamma_1 X - \omega R - \Lambda R \end{aligned} \tag{12}$$

Given that $R_0 \leq 0$, all of the eigenvalues are negative. Nevertheless, the following is how the fundamental reproduction number R_0 was obtained using the next-generation matrix approximations:

$$R_X = \frac{\beta_1}{\gamma_1 + \mu_1 + \delta_1} \tag{13}$$

2.3. Covid-19 Sub-model. When $(X = 0, Z = 0)$, Lassa fever is absent, the model simplifies to the Covid-19 sub-model, which is given by:

$$\begin{aligned} \frac{dS}{dt} &= \Lambda + \omega R - \frac{\beta_2 S(Y)}{S+Y+R} - \mu S \\ \frac{dY}{dt} &= \frac{\beta_2 S(Y)}{S+Y+R} - \gamma_2 Y - \mu Y - \delta_2 Y \\ \frac{dR}{dt} &= \gamma_2 Y - \omega R - dR \end{aligned} \tag{14}$$

The basic reproduction number R_0 was found using the next-generation matrix techniques, despite the fact that all of the eigenvalues are negative.

$$R_Y = \frac{\beta_2}{\gamma_2 + \mu + \delta_2} \tag{15}$$

2.4. Model of Lassa Fever and COVID-19 Co-infection. From equation (1) the new infection matrix F is

$$F = \begin{vmatrix} \beta_1 \frac{S_0}{N} & 0 & \beta_1 \frac{S_0}{N} \\ 0 & \beta_2 \frac{S_0}{N} & \beta_2 \frac{S_0}{N} \\ 0 & 0 & 0 \end{vmatrix} \tag{16}$$

The transition matrix V is defined as follows

$$V = \begin{vmatrix} \mu+\gamma_2+\delta_2 & 0 & -\gamma_2 \\ 0 & \mu+\gamma_2+\delta_2 & -\gamma_1 \\ 0 & 0 & \delta_1+\delta_2+\gamma_2+\gamma_1+\mu \end{vmatrix} \tag{17}$$

The basic reproduction number R_0

$$R_0 = \rho(FV^{-1})$$

$$k = FV^{-1}$$

$$k = \begin{vmatrix} \frac{\beta_1}{\mu_1+\gamma_1+\delta_1} & 0 & \frac{\beta_1}{\mu+\gamma_1+\delta_1} \\ 0 & \frac{\beta_2}{\mu+\gamma_2+\delta_2} & \frac{\beta_2}{\mu+\gamma_2+\delta_2} \\ 0 & 0 & 0 \end{vmatrix} \tag{18}$$

Eigenvalues

$$\lambda_1 = \frac{\beta_1}{\mu+\gamma_1+\delta_2} \qquad \lambda_3 = 0 \qquad \lambda_2 = \frac{\beta_2}{u+\gamma_2+\delta_2}$$

$$R_0 = max\left(\frac{\beta_1}{\mu+\gamma_1+\delta_1}, \qquad \frac{\beta_2}{\mu+\gamma_1+\delta_2}, \qquad 0\right)$$

The R_X and R_Y in equation (12) and equation (15) are important threshold quantities that are utilised to determine if the issue is endemic. For the system's of equations (1), R_0 is fundamental reproduction number. It gives maximum at R_X and R_Y.

$$R_0 = max\left[\frac{\beta_1}{\gamma_1+\mu+\delta_1}, \frac{\beta_2}{\gamma_2+\mu+\delta_2}\right] \tag{19}$$

If this threshold quantity ($R_0 > 1$) is bigger than unity, the co-epidemic will continue in the society.

3. Qualitative Analysis

Quantitative analysis of the modelled system of equations will be conducted to ascertain the system's long-term behaviour. To achieve this, a thorough analysis of the dynamics of the Lassa fever component model and the COVID-19 component model will be conducted to gain insights into understanding the overall co-epidemic model dynamics.

3.1. Equilibrium Free of Disease. The equilibrium free of disease is reached when no individuals in the community are infected with Lassa fever, COVID-19, or both diseases. Mathematically, this is determined by setting the derivatives in the model equations to zero and solving for the dependent variables simultaneously.

The disease free equilibrium for Lassa fever sub-model

$$\Sigma_{0X} = \left(\frac{\Lambda}{\mu},\ 0,\ 0\right) \tag{20}$$

The disease free equilibrium for Covid-19 sub-model only.

$$\Sigma_{0Y} = \left(\frac{\Lambda}{\mu},\ 0,\ 0\right) \tag{21}$$

The disease free equilibrium for both Lassa fever and Covid-19 full model is

$$\Sigma_0 = \left(\frac{\Lambda}{\mu},\ 0,\ 0,\ 0,\ 0\right) \tag{22}$$

The disease-free equilibrium provides specific conditions under which Lassa fever or COVID-19 will either die out or persist in the population.

3.2. Local Disease Equilibrium Stability.

Theorem 2. The disease free equilibrium E_{0X} for Lassa fever sub-model is locally asymptotically stable if $R_0 < 1$; otherwise it is unstable.

Proof: From the Lassa fever sub-model in equation 23 we obtain the Jacobian matrix of the system.

$$J_X = \begin{vmatrix} \frac{\beta_1 X}{S+X+R} + \frac{\beta_1 SX}{(S+X+R)^2} - \mu & \frac{\beta_1 S}{S+X+R} + \frac{\beta_1 S}{(S+X+R)^2} & \omega + \frac{\beta_1 SX}{(S+X+R)^2} \\ \frac{\beta_1 X}{S+X+R} - \frac{\beta_1 SX}{(S+X+R)^2} & \frac{\beta_1 S}{S+X+R} - \frac{\beta_1 SX}{(S+X+R)^2} - Y_1 - \mu - \delta_1 & \frac{-\beta_1 SX}{(S+X+R)^2} \\ 0 & Y_1 & -d-\omega \end{vmatrix} \tag{23}$$

Evaluating matrix [J_X at d.f.e $S = \frac{\Lambda}{\mu}$, $S = 0$, $R = 0$].

$$J_{OX} = \begin{vmatrix} -\mu & \beta_1 & \omega \\ 0 & \beta_1 - \mu - \delta_1 - \gamma_1 & 0 \\ 0 & \gamma_1 & -\delta - \omega \end{vmatrix} \tag{24}$$

$$J_{OX} = \begin{vmatrix} -\mu-\lambda & -\beta_1 & -\omega \\ 0 & \beta_1-\mu-\delta_1-\gamma_1-\lambda & 0 \\ 0 & \gamma_1 & -\delta-\omega-\lambda \end{vmatrix} \tag{25}$$

$$-\mu-\lambda[(\beta_1-\mu-\delta_1-\gamma_1-\lambda)(-\delta-\omega-\lambda)-\beta_1(0)]+0 \tag{26}$$

$$\lambda_1=-\mu,\lambda_2=-(\mu+\delta_1+\gamma_1-\beta_1),\lambda_3=-\delta_1-\omega \tag{27}$$

$$\lambda_1=-\mu_1 \qquad \lambda_2=-\mu-\delta+\beta_1-Y, \qquad \lambda_3=-\delta-\omega$$

Since all the eigenvalues are of the Jacobian matrix evaluated at E_{OX} have negative real parts, whenever $R_X<1$, then E_{0X} is locally asymptotically stable.

The disease free equilibrium for Lassa fever E_{0X} sub-model is locally asymptotically stable if $R_X<1$ while it is unstable otherwise.

Theorem 3. The disease free equilibrium E_{0Y} for the Covid-19 sub-model is locally asymptotically stable if $R_Y<1$; otherwise it is unstable.

Proof: From the Covid-19 sub-model system of equation in equation (14).

$$J_Y = \begin{vmatrix} \frac{-\beta_2 Y}{S+Y+R}+\frac{\beta_2 SY}{(S+Y+R)^2}-\mu & \frac{\beta_2 S}{S+Y+R}+\frac{\beta_2 SY}{(S+Y+R)^2} & \omega+\frac{\beta_2 SY}{(S+Y+R)^2} \\ \frac{\beta_2 Y}{S+Y+R}-\frac{\beta_2 SY}{(S+Y+R)^2} & \frac{\beta_2 S}{S+Y+R}-\frac{\beta_2 SY}{(S+Y+R)^2}-\gamma_2-\mu-\delta_2 & \frac{\beta_2 SY}{(S+Y+R)^2} \\ 0 & \gamma_2 & -\delta-\omega \end{vmatrix} \tag{28}$$

Evaluating matrix J_Y at d.f.e

$$\left(S=\frac{\Lambda}{\mu},Y=0,R=0\right)$$

$$J_{OY}\begin{vmatrix} \mu & -\beta_2 & \omega \\ 0 & -\mu+\beta_2-\delta_2-\gamma_2 & 0 \\ 0 & \gamma_2 & \delta-\omega \end{vmatrix} \tag{29}$$

$$J_O = \begin{vmatrix} \mu-\lambda & \beta_2 & \omega \\ 0 & -\mu+\beta_2-\delta_2-\gamma_2-\lambda & 0 \\ 0 & \gamma_2 & -\delta-\omega-\lambda \end{vmatrix} \tag{30}$$

$$-\mu-\lambda\left[(-\mu+\beta_2\delta_2-Y-\lambda)(-\delta-\omega-\lambda)--\beta_2(0-0)+\omega(0)\right] \tag{31}$$

Hence

$$\lambda_1=-\mu_1$$

$$\lambda_2=-\mu+\beta_2-\delta_2-\gamma_2=-(\mu-\beta_2+\delta_2+\gamma_2)$$

$$\lambda_3=-\delta-\omega$$

Since all the eigenvalues are negative for Jacobian matrix for E_{0Y} sub-model. It then have a negative real part whenever $R_Y<1$; then E_{0Y} is locally asymptomatically stable.

The disease free equilibrium for E_{0Y} is locally asymptotically stable for the Covid-19 if $R_Y<1$ or otherwise it is not stable.

Theorem 4. The disease free equilibrium for the full model for Lassa fever and Covid-19 co-epidemic model is locally asymptotically stable if $R_O<1$; otherwise it is unstable.

Proof: From the full model, that is equations (1) system of equations. The Jacobian matrix J is

$$J=\begin{vmatrix} \mu & -\beta_1\frac{S_0}{N} & -\beta_2\frac{S}{N} & -(\beta_1+\beta_2)\frac{S_0}{N} \\ 0 & \beta_1\frac{S_0}{N}--(\mu+\gamma_1+\delta_1) & 0 & \beta_1\frac{S_0}{N} \\ 0 & 0 & \beta_2\frac{S-0}{N}-(\mu+\gamma_2+\delta_2) & \beta_2\frac{S_0}{N} \\ 0 & \beta_2\frac{X}{\mu} & \beta_1\frac{\gamma_1}{N} & (\delta_1+\omega_2+\gamma_2+\gamma_1+\mu) \\ 0 & \gamma_1 & \gamma_2 & 0 \end{vmatrix} \tag{32}$$

Evaluating $S_0=\frac{\Lambda}{\mu}$

$$J_Z=\begin{vmatrix} -\mu & \beta_1\frac{\Lambda}{\mu N} & -\beta_2\frac{\Lambda}{\mu N} & -(\beta_1+\beta_2)\frac{\Lambda}{\mu N} \\ 0 & \beta_1\frac{\Lambda}{\mu N}-(\mu+\gamma_1+\delta_1) & 0 & \beta_1\frac{\Lambda}{\mu N} \\ 0 & 0 & \beta_2\frac{\Lambda}{\mu N}-(\mu+\gamma_2+\delta_2) & \beta_2\frac{\Lambda}{\mu N} \\ 0 & 0 & 0 & -(\delta_1+\delta_2+\gamma_2+\gamma_1+\mu) \\ 0 & \gamma_1 & \gamma_2 & 0 \end{vmatrix} \tag{33}$$

The eigenvalues are

$$\lambda_1=-\mu,\qquad \lambda_2=\beta_1\frac{S_0}{N}-(\mu+\gamma_1+\delta_1),\qquad \lambda_3=\beta_2\frac{S_0}{N}-(\mu+\gamma_2+\delta_2)$$

$$\lambda_4 = -(\delta_1 + \delta_2 + \gamma_2 + \gamma_1 + \mu), \qquad \lambda_5 = -(\omega + \delta)$$

Since all the eigenvalues are negative for Jacobian matrix, for Σ_{0z} full model. It then have a negative real part whenever $R_Z < 1$; then Σ_{0z} is local asymptotically stable.

The disease free equilibrium for Σ_{0z} for Covid-19 and Lassa fever are locally asymptotically stable if $R_z < 1$, or otherwise it is not stable.

3.3. Global Stability of Disease Equilibrium. By using the Lyapunov function technique to the component model equations, the global stability of the disease-free equilibrium will be determined. (12) and (14).

Theorem 5. The disease free equilibrium $\Sigma_{0X} = \left(\frac{\Lambda}{\mu},\ 0,\ 0\right)$ are, in turn, globally asymptomatic stable whenever $R_X < 1$, and $R_Y < 1$.

Proof: Using Lyapunov Function on Lassa fever equation only (12).

$$V(X,\ R) = X + \frac{R}{k} \tag{34}$$

where k is a positive constant

$$\frac{dV}{dt} = \frac{dx}{dt} + \frac{1}{k}\frac{dR}{dt} \tag{35}$$

$$\frac{dV}{dt} = \left[\beta_1 X\frac{S}{N} - (\mu + \gamma_1 + \delta_1)X\right] + \frac{1}{k}(\gamma_1 X - \omega + \delta R) \tag{36}$$

$$\frac{dV}{dt} = \left(\beta_1 X\frac{S}{N} - (\mu + \gamma_1 + \delta_1)X + \frac{\gamma_1 X}{k} - \frac{(\omega + \delta)R}{k}\right) \tag{37}$$

$S = S_0 = \frac{\Lambda}{\mu}$ near the DFE

$$\begin{aligned}\frac{dV}{dt} &= X\left(\beta_1\frac{S_0}{N} - \mu - \gamma_1 - \delta_1 + \frac{\gamma_1}{k}\right) - \frac{(\omega + \delta)R}{k} \\ &= X\left(\beta_1\frac{\Lambda}{\mu N} - \mu - \gamma_1 - \delta_1 + \frac{\gamma_1}{k}\right) - \frac{(\omega + \delta)R}{k}\end{aligned} \tag{38}$$

$$\beta_1\frac{\Lambda}{\mu N} - \mu - \gamma_1 - \delta_1 + \frac{\gamma_1}{k} \leq 0$$

$$\frac{\gamma_1}{k} \leq \mu + \gamma_1 + \delta_1 - \beta_1\frac{\Lambda}{\mu N}$$

$$\text{set } k \geq \frac{\gamma_1}{\mu + \gamma_1 + \delta_1 - \beta_1 \frac{\Lambda}{\mu N}}$$

$$\frac{dV}{dt} \leq 0$$

Thus proofing that the global stability of the disease free equilibrium.

To determine for global stability of disease equilibrium for Covid-19 only sub-model equation (14).

$$V(Y,\ R) = Y + \frac{R}{k}$$

$$\frac{dV}{dt} = \frac{dy}{dt} + \frac{1}{k}\ \frac{dR}{dt}$$

$$\frac{dV}{dt} = \left[\beta_2\ Y\frac{S}{N} - (\mu + \gamma_2 + \delta_2)Y\right] + \frac{1}{k}\left[\gamma_2 Y - (\omega + d)R\right] \tag{39}$$

$$\frac{dV}{dt} = Y(\beta_2\frac{S}{N} - \mu - \gamma_2 - \delta_2) + \gamma_2\frac{Y}{k} - \frac{(\omega + d)R}{k}$$

$S = S_0 = \frac{\Lambda}{\mu}$

$$\frac{dV}{dt} = Y\left(\beta_2\frac{\Lambda}{\mu N} - \mu - \gamma_2 - \delta_2 + \frac{\gamma_2}{k}\right) - \frac{(\omega + d)R}{k}$$

$$\frac{\gamma_2}{k} \leq \mu + \gamma_2 + \delta_2 - \beta_2\frac{\Lambda}{\mu N}$$

$$k \geq \frac{\gamma_2}{\mu + \gamma_2 + \delta_2} - \beta_2\frac{\Lambda}{\mu N}$$

$\frac{dV}{dt} \leq 0$. This show the global stability of the Covid-19 sub-model. It is important to note that V = 0 provided x = 0 and y = 0 in equations (35) and (39). Therefore the global stability of Σ_0 whenever $R_x < 1$ and $R_y < 1$ follow from Lascelles invariance principle [**?**].

Theorem 6. The disease free equilibrium $\Sigma_{0z} = \left(\frac{\Lambda}{\mu},\ ,\ 0,\ 0,\ 0,\ 0\right)$ whenever $R_z < 1$ is globally asymptomatically stable.

Proof: Let us consider olympunous function of the form

$$V(S,\ X,\ Y,\ Z,\ R) = S + X + Y + Z + \frac{R}{k}$$

Where k is a positive constant.

$$\frac{dV}{dt} = \frac{dS}{dt} + \frac{dX}{dt} + \frac{dY}{dt} + \frac{dZ}{dt} + \frac{1}{k}\ \frac{dR}{dt}$$

$$\frac{dV}{dt} = \left[\beta_1(X+Z)\frac{S}{N} - \beta_2(Y+Z)\frac{X}{N} - (\mu+\gamma_1+\delta_1)X + \gamma_2 Z\right]$$
$$+ \left[\beta_2(Y+Z)\frac{S}{N} - \beta_1(X+Y)\frac{Y}{N} - (\mu+\gamma_2+\delta_2)Y + \gamma_1 Z\right]$$
$$+ \left[\beta_1(X+Z)\frac{Y}{N} + \beta_2(Y+Z)\frac{X}{N} - (\delta_1+\delta_2+\gamma_2+\gamma_1+\mu)Z\right]$$
$$+ \frac{1}{k}(\gamma_1 X + \gamma_2 Y - (\omega+\delta)R)$$

$$\frac{dV}{dt} = \beta_1(X+Z)\frac{S}{N} + \beta_2(Y+Z)\frac{S}{N} - (\mu+\gamma_1+\delta_1)X - (\mu+\gamma_2+\delta_2)Y - (\delta_1+\delta_2+\frac{\gamma_1}{k}X) + \frac{\gamma_2}{k}Y - \frac{\omega+\delta}{k}R$$

$S = S_0 = \frac{\Lambda}{\mu}$

$$\frac{dV}{dt} = (\mu+\gamma_1+\delta_1)X - (\mu+\gamma_2+\delta_2)Y - (\delta_1+\delta_2+\gamma_2+Y+\mu)Z - \frac{(\omega+\delta)R}{k}$$

$\frac{dV}{dt} \leq 0$. Since v is positively defined and v is only for Lyapunov function. Shows that the full model is global asymptotically stable for the disease free equilibrium.

3.4. Stable Endemic Solution. In the endemic equilibrium, the illness component consistently maintains positive values, creating a stable state. COVID-19, Lassa fever, and co-infections with COVID-19 are ubiquitous in society.

The Lassa fever sub-model's endemic model was created using the equations. (12)

$$\Sigma_X^* = \left[S^* = \frac{N(\mu+\gamma_1+\delta_1)}{\beta_1}, \quad X^* = \frac{\beta_1\Lambda - N\mu(\mu+\gamma_1+\delta_1)}{\beta_1(\mu+\gamma_1+\delta_1) - \frac{\omega\gamma_1}{\omega+\delta}}, \quad R^* = \frac{\gamma_1 X^*}{\omega+\delta}\right]$$

The endemic equilibrium solution for Covid-19 sub-model equation (**??** − **??**)

$$\Sigma_Y^* = \left[S^* = \frac{N(\mu+\gamma_2+\delta_2)}{\beta_2}, \quad Y^* = \beta_2\Lambda - \frac{N\mu(\mu+\gamma_2+\delta_2)}{\beta_2(\mu+\gamma_2+\delta_2)} - \frac{\omega\gamma_2}{\omega+\delta}, \quad R^* = \frac{\gamma_2 Y^*}{\omega+\delta}\right]$$

The evidence solution for the full co-infected model equation (1). Local stability of the evidence equilibrium.

$$\begin{aligned} S^* &= \frac{\Lambda+\omega R}{\beta_1(X^*+Z^*) + \beta_2\dfrac{Y^*+Z}{N}} + \mu \\ X^* &= \frac{\beta_1(X^*+Z^*)\dfrac{S^*}{N} + \gamma_2 Z}{\beta_2\frac{(Y^*+Z^*)}{N} + \mu + \gamma_1 + \delta_1} \\ Y^* &= \frac{\beta_2(Y^*+Z^*)\dfrac{S^*}{N} + \gamma_1 Z}{\beta_1\dfrac{(X^*+Y^*)}{N} + \mu + \gamma_2 + \delta_2} \end{aligned} \tag{40}$$

$$\begin{aligned} Z^* &= \frac{\beta_1(X^*+Z^*)\dfrac{Y^*}{N}+\beta_2(Y^*+Z^*)\dfrac{X^*}{N}}{1+\delta_2+\gamma_2+\gamma_1+\mu} \\ nmnR^* &= \frac{\gamma_1 X^*+\gamma_2 Y^*}{\omega+\delta} \end{aligned}$$

Theorem 7. The evidence equilibrium Σ_X^* for Lassa fever sub-model is locally asymptotically stable if $R_X > 1$.

Proof: The Lassa fever sub-model is linearised using Jacobian matrix approach and solve.

Evaluate the Jacobian at the endemic equilibrium. At the endemic equilibrium S^*, X^*, R^* we substitute $S = S^*, \quad X = X^*, \quad$ and $R = R^*$

$$J = \begin{vmatrix} -\beta_2 X^* \frac{1}{X} - \mu & -\beta_1 \frac{S^*}{N} & \omega \\ \beta_2 X^* \frac{1}{N} & \beta_2 \frac{S^*}{N} - (\mu+\gamma_2+\delta_1) & 0 \\ 0 & \gamma_1 & -(\omega+\delta) \end{vmatrix}$$

Substitute S^*, X^* and R^* into the Jacobian matrix and simplifying

$$J = \begin{vmatrix} \frac{-\beta_1\Lambda - N\mu(\mu+\gamma_1+\delta_1)}{N(\mu+\gamma_1+\delta_1)-\frac{-\omega\gamma_1}{\omega+\delta}} - \mu & -(\mu+\gamma_1+\delta_1) & \omega \\ \frac{\beta_1\Lambda - N(\mu+\gamma_1+\delta_1)}{N(\mu+\gamma_1+\delta_1)-\frac{-\omega\gamma_1}{\omega+\delta}} & 0 & 0 \\ 0 & \gamma_1 & -(\omega+\delta) \end{vmatrix} \tag{41}$$

The trace

$$(J) = \left[\frac{-\beta_1\Lambda - N\mu(\mu+\gamma_1+\delta_1)-\mu}{N(\mu+\gamma_1+\delta_1)-\frac{-\omega\gamma_1}{\omega+\delta}}\right] + 0 + (-\omega+\delta)$$

trace

$$J_X = \frac{-\beta_1\Lambda - N\mu(\mu+\gamma_1+\delta_1)-\mu}{N(\mu+\gamma_1+\delta_1)-\frac{-\omega\gamma_1}{\omega+\delta}} - \mu - (\omega+\delta)$$

The determinant of the matrix J_X det (J_X)

$$\det J_X = \frac{-\beta_1\Lambda - N\mu(\mu+\gamma_1+\delta_1)}{N(\mu+\gamma_1+\delta_1)-\frac{-\omega\gamma_1}{\omega+\delta}}\ (\mu+\gamma_1+\delta_1)(\omega+\delta) + \omega\gamma_1$$

The steady-state of an endemic Σ_X^* exhibits local asymptotic stability if $R_X > 1$ at provided $\gamma_1 > \mu_X$ The Jacobian matrix of the COVID-19 sub-model was derived and assessed at the

endemic equilibrium Σ_Y is given and simplified further.

$$J_Y = \begin{vmatrix} \frac{-\beta_2\Lambda - N\mu(\mu+\gamma_2+\delta_2)}{N(\mu+\gamma_2+\delta_2)-\frac{\omega\gamma_1}{\omega+\delta}} - \mu & -(\mu+\gamma_2+\delta_2) & \omega \\ \frac{-\beta_2\Lambda - N\mu(\mu+\gamma_2+\delta_2)}{N(\mu+\gamma_2+\delta_2)-\frac{\omega\gamma_1}{\omega+\delta}} - \mu & 0 & 0 \\ 0 & \gamma_2 & -(\omega+\delta) \end{vmatrix}$$

$$(J_Y) = \frac{-\beta_2\Lambda - N\mu(\mu+\gamma_2+\delta_2)}{N(\mu+\gamma_2+\delta_2)-\frac{\omega\gamma_2}{\omega+\delta}} - \mu - (\omega+\delta)$$

$$\text{deter}\,(J_Y) = \frac{-\beta_2\Lambda - N\mu(\mu+\gamma_2+\delta_2)}{N(\mu+\gamma_2+\delta_2)-\frac{\omega\gamma_2}{\omega+\delta}}\,((\mu+\gamma_2+\delta_2)(\omega+\delta)+\omega\gamma_2)$$

The endemic equilibrium of the COVID-19 sub-model Σ_Y^* demonstrates local asymptotic stability if $R_Y > 1$ provided $\beta_2 > \mu$.

3.5. Global Stability of the Endemic Equilibrium.

Theorem 8. If $R_X > 1$, then an endemic equilibrium Σ_X^* exists (in addition to the disease-free equilibrium), and it is globally asymptotically stable.

Proof: Given that $R_X > 1$, then the existence of the equilibrium is generated, considering a Lyapunov function for Lassa fever equations (12). The endemic equilibrium points are:

$$S^* = N\frac{(\mu+\gamma_1+\delta_1)}{\beta_1}, \quad X^* = \frac{-\beta_1\Lambda - N\mu(\mu+\gamma_1+\delta_1)}{\beta_1(\mu+\gamma_1+\delta_1)-\frac{\omega\gamma_1}{\omega+\delta}}, \quad R^* = \frac{\gamma_1 X^*}{\omega+\delta}$$

To prove global stability, we need to show that $\frac{dv}{dt} \leq 0$.

$$\frac{dv}{dt} = 2\omega_1\left(1-\frac{S^*}{S}\right)\frac{dS}{dt} + 2\omega_2\left(1-\frac{X^*}{X}\right)\frac{dX}{dt}$$

Substituting the expression for $\frac{dS}{dt}$ and $\frac{dX}{dt}$

$$\frac{dv}{dt} = 2\omega_1\left(1-\frac{S^*}{S}\right)\left(\Lambda+\omega R-\beta_1 X\frac{S}{N}-\mu S\right) + 2\omega_2\left(1-\frac{X^*}{X}\right)\left(\beta_1 X\frac{S}{N}-\mu S\right)$$

$$\frac{dv}{dt} = 2\omega_1\left(1-\frac{S^*}{S}\right)\left(\Lambda+\omega R-\beta_1 X\frac{S}{N}-\mu S\right)$$

Using the equilibrium conditions and Substituting

$$\Lambda+\omega R^* = \beta_1 X^*\frac{S^*}{N}+\mu S^*$$

$$= 2\omega_1\left(1-\frac{S^*}{S}\right)\left(\beta_1 X^*\frac{S^*}{N}+\mu S-\beta_1 X\frac{S}{N}-\mu S\right) + 2\omega_2\left(1-\frac{X^*}{X}\right)\left(\beta_1 X\frac{S}{N}-(\mu+\gamma_1+\delta_1)X\right)$$

Using the equilibrium condition and substituting

$$\beta_1 X^* \frac{S^*}{N} = (\mu + \gamma_1 + \delta_1)X^* + 2\omega_2 \left(1 - \frac{X^*}{X}\right)\left(\beta_1 X \frac{S}{N} - (\mu + \gamma_1 + \delta_1)X\right)$$

$$\frac{dv}{dt} = 2\omega_2 \left(1 - \frac{S^*}{S}\right)\left(\beta_1 X^* \frac{S^*}{N} + \mu S - \beta_1 X \frac{S}{N} - \mu S\right) + 2\omega_2 \left(1 - \frac{X^*}{X}\right)$$

As a result, the endemic equilibrium remain stable globally.

Theorem 9. If $R_Y > 1$, then an endemic equilibrium exists Σ_Y^* (alongside the disease-free equilibrium) and it is globally asymptotically stable.

Proof: Given that $R_Y > 1$, For the COVID-19 equation, the existence of the equilibrium is assured (14). The endemic equilibrium points are:

$$S^* = \frac{N(\mu + \gamma_2 + \delta_2)}{\beta_2}$$

$$Y^* = \frac{\beta_2 \Lambda - N\mu(\mu + \gamma_2 + \delta_2)}{\beta_2(\mu + \gamma_2 + \beta_2) - \frac{\omega\gamma_1}{\omega + \delta}}$$

$$R^* = \frac{\gamma_2 Y^*}{\omega + \delta}$$

$$V(S,\, Y,\, R) = 2\omega_1 \left(S - S^* - S^* ln\left(\frac{S}{S^*}\right)\right) + 2\omega_2 \left(Y - Y^* - Y^* ln\left(\frac{Y^*}{Y}\right)\right) + \left(R - R^* - R^* ln\left(\frac{R^*}{R}\right)\right)$$

$$\frac{dv}{dt} = 2\omega_1 \left(1 - \frac{S^*}{S}\right)\frac{dS}{dt} + 2\omega_1 \left(1 - \frac{Y^*}{Y}\right)\frac{dy}{dt}$$

Substituting the expression $\frac{dS}{dt}$ and $\frac{dy}{dt}$.

$$\frac{dv}{dt} = 2\omega_1 \left(1 - \frac{S^*}{S}\right)\left(\beta_2 Y^* \frac{S^*}{N} + \mu S^* - \beta_2 Y \frac{S}{N} - \mu S\right) + 2\omega_2 \left(1 - \frac{Y^*}{Y}\right)$$

The Lyapunov function V(S, Y, R) proves a way to show that $\frac{dv}{dt} \leq 0$. The endemic equilibrium for Covid-19 is globally stable.

Theorem 10. If $R_Z > 1$, for the full-model that cause infection of Lassa fever and Covid-19. Then there exist an endemic equilibrium Σ_Z and it exhibits global asymptotic stability.

Proof: Given that $R_Z > 1$, and considering a Lyapunov function, the existence of the equilibrium is assured.

$$V(S,\,X,\,Y,\,Z,\,R) = \left(S - S^* - S^* ln\left(\frac{S}{S^*}\right)\right) + 2\omega_2\left(X - X^* - S^* ln\left(\frac{X}{X^*}\right)\right)$$
$$+2\omega_2\left(Y - Y^* - S^* ln\left(\frac{Y}{Y^*}\right)\right) + 2\omega_1\left(Z - Z^* - Z^* ln\left(\frac{Z}{Z^*}\right)\right) + ...$$
$$\frac{dv}{dt} = 2\omega_1\left(1 - \frac{S^*}{S}\right)\frac{dS}{dt} + 2\omega_2\left(1 - \frac{X^*}{X}\right)\frac{dX}{dt} + 2\omega_2\left(1 - \frac{Y^*}{Y}\right)\frac{dY}{dt} + ...$$
$$\frac{dv}{dt} = 2\omega_1\left(1 - \frac{S^*}{S}\right)\left(\Lambda + \omega R - \beta_1(X+Z)\frac{S}{N} - \beta_2(Y+Z)\frac{S}{N} - \mu S\right)$$

$$\frac{dv}{dt} = 2\omega_1\left(1 - \frac{S^*}{S}\right)\left(\beta_1(X^*+Z^*)\frac{S^*}{N} + \beta_2(Y^*+Z^*)\right)$$
$$\frac{S^*}{N} + \mu S^* + \beta_1(Y+Z)\frac{X}{N} + 2\omega_2\left(1 - \frac{X^*}{X}\right)(\mu + \gamma_1 + \delta_1)X^* - \gamma_2 Z^* - \beta_2(Y+Z)\frac{X}{N}$$
$$-\mu X - \gamma_1 + 2\omega_3\left(1 - \frac{Y^*}{Y}\right)(\mu + \gamma_2 + \delta_2)Y^* - \gamma_1 Z - \beta_1(X+Y)$$
$$\frac{Y}{N} - \mu Y - \gamma_2 + 2\omega_1\left(1 - \frac{Z^*}{Z}\right)(\delta_1 + \delta_2 + \gamma_2 + \gamma_1 + \mu)Z^* - \beta_1(X+Z)\frac{Y}{N}$$
$$-\beta_2(Y+Z)\frac{Z}{N} + 2\omega S\left(1 - \frac{R^*}{R}\right)((\omega + \delta)R - \gamma_1 X - \gamma_2 Y - \omega\delta - \delta R)$$

$\frac{dv}{dt} \leq 0$

The Lyapunov function V(S, X, Y, Z, R) constructed in this manner ensures that $\frac{dv}{dt} \leq 0$, thereby confirming the global stability of the endemic equilibrium.

4. Sensitivity Analysis

Sensitivity analysis will be conducted to assess how the basic reproduction number R_0 responds to variations in each model parameter. We will use the Normalized Forward-Sensitivity Index (NFSI), which is calculated by multiplying the partial derivative of R_0 with respect to each parameter by the ratio of the parameter to R_0.

$\beta_1 : \Longrightarrow \frac{\partial R_0}{\partial \beta} \times \frac{\beta}{R_0} = 1$, $\delta_1 : \Longrightarrow \frac{\partial R_0}{\partial \delta} \times \frac{\delta}{R_0} = \left(\frac{-\delta}{\gamma_1+\mu+\delta_1}\right) = -0.0396$, $\gamma_1 : \Longrightarrow \frac{\partial R_0}{\partial \gamma} * \frac{\gamma}{R_0} = \left(\frac{-\delta}{\gamma_1+\mu+\delta_1}\right) = -0.06602$, $\mu_1 : \Longrightarrow \frac{\partial R_0}{\partial \mu} \times \frac{\mu}{R_0} = \left(\frac{-\delta}{\gamma_1+\mu+\delta_1}\right) = -0.3001$, $\beta_2 : \Longrightarrow \frac{\partial R_0}{\partial \beta} \times \frac{\beta}{R_0} = 1$, $\delta_2 : \Longrightarrow \frac{\partial R_0}{\partial \delta_2} \times \frac{\delta_2}{R_0} = \left(\frac{-\delta_2}{\gamma_2+\mu_2+\delta_2}\right) = -0.928$, $\gamma_2 : \Longrightarrow \frac{\partial R_0}{\partial \gamma_2} * \frac{\gamma_2}{R_0} = \left(\frac{-\gamma_2}{\gamma_2+\mu_2+\delta_2}\right) = -0.072$, $\mu_2 : \Longrightarrow \frac{\partial R_0}{\partial \mu_2} \times \frac{\mu}{R_0} = \left(\frac{-\mu_2}{\gamma_2+\mu_2+\delta_2}\right) = -0.0000112$.

Table 3 presents the sensitivity indices of R_0 with respect to each model parameter.

The values in the table above indicate the impact on R_0 when a parameter is increased or decreased. R_0 rises when the sensitivity indices with positive signs increase, and it falls when the sensitivity indices with negative signs increase, and vice versa. The parameters most sensitive to R_x and R_y are identified as β_1 and β_2.

TABLE 3. Sensitivity Indices of R_0 to Parameters

Parameter	**Parameter Description**	**Sensitivity Index**
β_1	Transmission rate of Lassa fever	1
β_2	Transmission rate of Covid19	1
δ_1	Disease induced death rate for Lassa fever	-0.0396
δ_2	Disease induced death rate for Covid19	-0.928
μ_1	Natural death rate of human during Lassa	-0.3001
μ_2	Natural death rate of human during Covid19	-0.0000112
γ_1	Recovery rate for Lassa fever	-0.6602
γ_2	Recovery rate for Covid19	-0.072

4.1. Results and Discussion of Numerical Analysis. The values in the table 3 illustrate the impact on R_0 when a parameter is increased or decreased. R_0 rises when the sensitivity indices with positive signs increase, and it falls when the sensitivity indices with negative signs increase, and vice versa. The parameters most sensitive to R_x and R_y are identified as β_1 and β_2.

The value in Table 3 illustrate the impact on R_0 when the parameter is varied. An increase in sensitivity indices with a positive sign leads to an increase in R_0, whereas an increase in sensitivity indices with a negative sign results in a decrease in R_0, and vice versa. The parameters β_1 and β_2 are identified as the most sensitive to R_x and R_y, respectively.

The susceptible graph indicates that the red line represents $R_0 > 1$, signifying the presence of the disease in the system. As long as the disease persists, the susceptible population will decrease. Conversely, once the disease is eradicated, the susceptible population will begin to increase.

The Lassa infected graph shows that the red line represents $R_0 > 1$, indicating the presence of Lassa Fever in the system. As a result, the susceptible population is exposed to Lassa Fever and becomes infected, leading to an increase in the Lassa infected population.

The graph indicates that the number of infected individuals will continue to rise if control measures are not implemented. However, with effective control measures in place and $R_0 < 1$, the number of infected individuals will decrease.

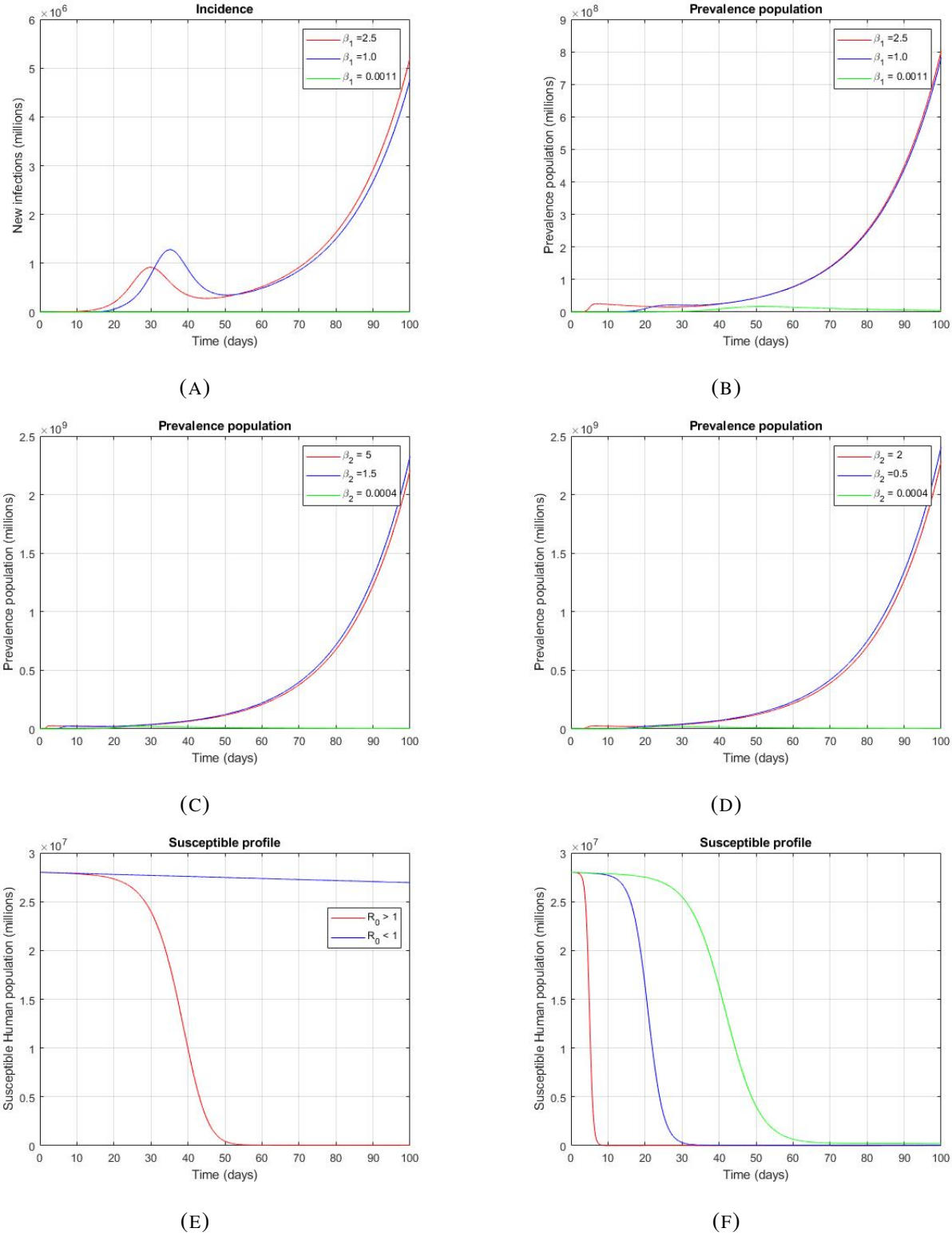

FIGURE 2. (a) Susceptible (b) Covid-19 (c) Population profile for the model compartments (d) New Cases and Prevalence of Lassa fever Disease Plots (e) Susceptible profile

TABLE 4. Description of the model's parameters

Parameter	**Description**	**Value**	**unit**	**Source**
Λ,	Recruitment rate	0.3465	per day	[27]
β_1	Transmission rate of Lassa fever	0.048	per day	[27]
β_2	Transmission rate of Covid-19	2.55	per day	[28]
δ_1	Disease induced death rate for Lassa fever	0.0396	per day	[29]
δ_2	Disease induced death rate for Covid19	3.5	per day	[28]
μ_1	Natural death rate of human during Lassa	0.018182	per day	[30]
μ_2	Natural death rate of human during Covid19	0.0000421	per day	[28]
γ_1	Recovery rate for Lassa fever	0.04	per day	Estimated
γ_2	Recovery rate for Covid19	0.27	per day	[28]

The Covid-19 infected graph shows that the red line represents $R_0 > 1$, indicating the presence of Covid-19 in the system. Consequently, the susceptible population is exposed to Covid-19 and becomes infected, leading to an increase in the Covid-19 infected population.

The graph indicates that the number of infected individuals will continue to rise as long as the susceptible population keeps coming into contact with infected people. However, with effective control measures in place and implemented, $R_0 < 1$ will drop below 1, leading to a decrease in infections.

The co-infected graph shows that the red line represents $R_0 > 1$, indicating the presence of both Lassa Fever and Covid-19 in the system. Consequently, the susceptible population is exposed to both diseases and becomes infected, leading to an increase in the co-infected population.

The graph indicates that the number of infected individuals will continue to rise as long as the susceptible population keeps coming into contact with infected people. However, with effective control measures in place and implemented, $R_0 < 1$ will drop below 1, leading to a decrease in infections.

The recovered graph shows that when $R_0 > 1$, indicating the disease is widespread in the system, prompt treatment and the implementation of control measures will enhance recovery and increase the recovered population. However, when $R_0 < 1$, there are neither new infections nor recoveries.

The variation in the transmission rate of the disease indicates the rate at which new cases of Lassa Fever are emerging in the environment.

The graph indicates that the number of infected individuals will continue to rise as long as the susceptible population keeps coming into contact with infected people. However, with effective control measures in place and implemented, no new cases will emerge.

The prevalence graph indicates that the number of infected individuals will continue to rise as long as the susceptible population keeps coming into contact with infected people, leading to the prevalence of Lassa Fever in the environment. However, with effective control measures in place and implemented, no new cases will emerge, preventing the prevalence of the disease.

The variation in the transmission rate of the disease indicates the rate at which new cases of Covid-19 are being generated in the environment.

The graph indicates that the number of infected individuals will continue to rise as long as the susceptible population keeps coming into contact with infected people. However, with effective control measures in place and implemented, no new cases will occur.

The prevalence graph indicates that the number of infected individuals will continue to rise as long as the susceptible population keeps coming into contact with infected people, leading to the prevalence of Covid-19 in the environment. However, with effective control measures in place and implemented, no new cases will emerge, preventing the prevalence of the disease.

4.2. Conclusion. In conclusion, the rising prevalence of co-infections with Lassa fever (LF) and COVID-19, due to their similar transmission modes, underscores the urgent need for effective control measures to prevent a co-epidemic. Despite the availability of a COVID-19

vaccine, the absence of a vaccine for LF heightens the risk. This study presents a deterministic model for LF and COVID-19, emphasizing the critical consequences that must be addressed to mitigate the challenges of a co-epidemic. Through qualitative analysis, the basic reproduction number R_0 is derived, and stability criteria for each model equilibrium are established. Numerical solutions and simulations for various co-epidemic scenarios are provided, with the results thoroughly discussed.

CONFLICT OF INTERESTS

The authors declare that there is no conflict of interests.

REFERENCES

[1] R. Peckham, The Chronopolitics of Covid-19, Am. Lit. 92 (2020), 767–779. https://doi.org/10.1215/00029831-8780983.

[2] W.G. Carlos, C.S. Dela Cruz, B. Cao, et al. COVID-19 Disease Due to Sars-Cov-2 (Novel Coronavirus), Am. J. Respir. Crit. Care Med. 201 (2020), 7–8. https://doi.org/10.1164/rccm.2014p7.

[3] A. Duvignaud, M. Jaspard, I.C. Etafo, et al. Lassa Fever Outcomes and Prognostic Factors in Nigeria (LASCOPE): A Prospective Cohort Study, Lancet Glob. Heal. 9 (2021), e469–e478. https://doi.org/10.1016/s2214-109x(20)30518-0.

[4] M.E. Ogbole, J.A. Ameh, S. Mailafia, O.H. Olabode, B.J. Adah, Occurrence of Lassa Fever Virus Infections and Control Efforts in Nigeria, Hosts Viruses 9 (2022), 26–34. https://doi.org/10.17582/journal.hv/2022/9.1.7.11.

[5] I. Nwafia, M. Ohanu, Lassa Fever: Time to Eradicate the Deadly Disease in Nigeria, Niger. J. Clin. Pract. 22 (2019), 144. https://doi.org/10.4103/njcp.njcp_116_18.

[6] I.O. Eranga, Covid-19 Pandemic in Nigeria: Palliative Measures and the Politics of Vulnerability, Int. J. Matern. Child Heal. AIDS 9 (2020), 220–222. https://doi.org/10.21106/ijma.394.

[7] M. Okereke, E. Fortune, A.O. Peter, et al. Second Wave of COVID-19 in Nigeria: Lessons from the First Wave, Int. J. Heal. Plan. Manag. 37 (2021), 650–656. https://doi.org/10.1002/hpm.3396.

[8] M. Adeiza, S. Chinenye, Lassa Fever in West Africa: A 50-Year Review, J. Liber. Med. Dent. Assoc. 19 (2019), 40–50.

[9] B.D. Loomis, D. Felikson, T.J. Sabaka, B. Medley, High-spatial-resolution Mass Rates From Grace and Grace-fo: Global and Ice Sheet Analyses, J. Geophys. Res.: Solid Earth 126 (2021), e2021JB023024. https://doi.org/10.1029/2021jb023024.

[10] J. Gund, L.V.R. De Aruda, F.N. Junior, Comparative Analysis Between Two Convolutional Neural Networks Structures Applied to a Small Steel Surface Defects Database, in: 2021 14th IEEE International Conference on Industry Applications (INDUSCON), IEEE, São Paulo, Brazil, 2021: pp. 655–660. https://doi.org/10.1109/INDUSCON51756.2021.9529819.

[11] I.S. Lukashevich, The Search for Animal Models for Lassa Fever Vaccine Development, Expert Rev. Vaccines 12 (2013), 71–86. https://doi.org/10.1586/erv.12.139.

[12] E. Fichet-Calvet, E. Lecompte, L. Koivogui, et al. Fluctuation of Abundance and Lassa Virus Prevalence in Mastomys Natalensis in Guinea, West Africa, Vector-Borne Zoonotic Dis. 7 (2007), 119–128. https://doi.org/10.1089/vbz.2006.0520.

[13] A.A. Cunningham, P. Daszak, J.L.N. Wood, One Health, Emerging Infectious Diseases and Wildlife: Two Decades of Progress?, Philos. Trans. R. Soc. B: Biol. Sci. 372 (2017), 20160167. https://doi.org/10.1098/rstb.2016.0167.

[14] WHO, Progress and future directions of WHO respiratory syncytial virus surveillance – Report from the WHO meeting in November 2022, World Health Organization, 2023. https://iris.who.int/handle/10665/366859.

[15] B.H. Gulumbe, U. Aminu, U.U. Liman, et al. Recurring Outbreaks of Lassa Fever in Nigeria: Understanding the Root Causes and Strategies for the Future, Sudan J. Med. Sci. 18 (2023), 257–264.

[16] H.B. Taboe, K.V. Salako, J.M. Tison, C.N. Ngonghala, R. Glèlè Kakaï, Predicting Covid-19 Spread in the Face of Control Measures in West Africa, Math. Biosci. 328 (2020), 108431. https://doi.org/10.1016/j.mbs.2020.108431.

[17] E. Sherrard-Smith, A.B. Hogan, A. Hamlet, et al. The Potential Public Health Consequences of Covid-19 on Malaria in Africa, Nat. Med. 26 (2020), 1411–1416. https://doi.org/10.1038/s41591-020-1025-y.

[18] S.S. Musa, S. Zhao, Z.U. Abdullahi, A.G. Habib, D. He, COVID-19 and Lassa Fever in Nigeria: a Deadly Alliance?, Int. J. Infect. Dis. 117 (2022), 45–47. https://doi.org/10.1016/j.ijid.2022.01.058.

[19] B. Sivakumar, Chaos in Hydrology, Springer, (2016).

[20] A.T. Rabiu, A. Mohan, S. Çavdaroğlu, et al. Dengue and Covid-19: a Double Burden to Brazil, J. Med. Virol. 93 (2021), 4092–4093. https://doi.org/10.1002/jmv.26955.

[21] S. Jain, I.C.N. Rocha, C. Maheshwari, A.C.D. Santos Costa, C. Tsagkaris, A.T. Aborode, M.Y. Essar, S. Ahmad, Chikungunya and COVID-19 in Brazil: the Danger of an Overlapping Crises, J. Med. Virol. 93 (2021), 4090–4091. https://doi.org/10.1002/jmv.26952.

[22] A.C.D.S. Costa, M.M. Hasan, E. Xenophontos, et al. COVID-19 and Zika: an Emerging Dilemma for Brazil, J. Med. Virol. 93 (2021), 4124–4126. https://doi.org/10.1002/jmv.27006.

[23] S. Çavdaroğlu, M.M. Hasan, A. Mohan, et al. The Spread of Yellow Fever Amidst the COVID-19 Pandemic in Africa and the Ongoing Efforts to Mitigate It, J. Med. Virol. 93 (2021), 5223–5225. https://doi.org/10.1002/jmv.27027.

[24] A.N. Happi, C.T. Happi, R.J. Schoepp, Lassa Fever Diagnostics: Past, Present, and Future, Curr. Opin. Virol. 37 (2019), 132–138. https://doi.org/10.1016/j.coviro.2019.08.002.

[25] C. Ojide, E. Kalu, E. Ogbaini-Emevon, V. Nwadike, Coinfectionss of Hepatitis B and C with Human Immunodeficiency Virus Among Adult Patients Attending Human Immunodeficiency Virus Outpatients Clinic in Benin City, Nigeria, Niger. J. Clin. Pr. 18 (2015), 516–521. https://doi.org/10.4103/1119-3077.151790.

[26] E.F. Long, N.K. Vaidya, M.L. Brandeau, Controlling Coepidemicss: Analysis of HIV and Tuberculosis Infection Dynamics, Oper. Res. 56 (2008), 1366–1381. https://doi.org/10.1287/opre.1080.0571.

[27] N. Chitnis, J.M. Hyman, J.M. Cushing, Determining Important Parameters in the Spread of Malaria Through the Sensitivity Analysis of a Mathematical Model, Bull. Math. Biol. 70 (2008), 1272–1296. https://doi.org/10.1007/s11538-008-9299-0.

[28] F. Ndaïrou, D.F.M. Torres, Mathematical Analysis of a Fractional COVID-19 Model Applied to Wuhan, Spain and Portugal, Axioms 10 (2021), 135. https://doi.org/10.3390/axioms10030135.

[29] J.O. Agbomola, A.C. Loyinmi, Modelling the Impact of Some Control Strategies on the Transmission Dynamics of Ebola Virus in Humanbatt Population: an Optimal Control Analysis, Heliyon 8 (2022), e12121. https://doi.org/10.1016/j.heliyon.2022.e12121.

[30] Y. Nazir, S.A. Hussain, A. Abdul Hamid, Y. Song, Probiotics and Their Potential Preventive and Therapeutic Role for Cancer, High Serum Cholesterol, and Allergic and HIV Diseases, BioMed Res. Int. 2018 (2018), 3428437. https://doi.org/10.1155/2018/3428437.